Open-Loop Vibration Control of an Underwater System: Application to Refueling Machine

Umer Hameed Shah, *Student Member, IEEE*, Keum-Shik Hong, *Senior Member, IEEE*, and Sang-Hei Choi

***Abstract*—This paper addresses a residual vibration control problem of the refueling machine (RM) that transports fuel rods in water to their desired locations in the nuclear reactor. A hybrid lumped-mass and distributed-parameter model of the RM is considered for investigation of the transverse vibrations (caused by trolley movement) of a fuel rod in water. Simulations and experiments reveal that the hydrodynamic force causes a large deflection of the rod in water as compared with in air, which must be suppressed to avoid damage to the rod's fissile material. A new command-shaping method for suppression of the flexible rod's residual vibrations in water is developed, which considers both a similitude law relating the maximum endpoint deflection of the rod in water to the maximum trolley velocity and a constraint on the rod's maximum endpoint deflection during its transport. The simulation and experimental results show that the proposed underwater-command-shaping method can effectively suppress the vibrations of the flexible rod operating in water.**

***Index Terms*—Flexible system, fluid–structure interaction, input shaping, nuclear power plant, refueling machine (RM), underwater (UW) system, vibration control.**

I. Introduction

THIS PAPER discusses the vibration control problem of the refueling machine (RM) in a nuclear power plant [1]. The RM, a type of overhead crane, transports nuclear fuel rods to their desired reactor locations in water (to minimize radiation leaks to the environment). During a maintenance period, quick transference of fuel rods is essential to the economical operation of the power plant. However, quick maneuvering of a fuel rod in water can generate a hydrodynamic force, causing a large deflection that can damage the fissile material within [2]. Certainly, insertion of a damaged fuel rod into the reactor core incurs a very serious safety hazard [3]. Therefore, the objective of this paper is to develop an appropriate control strategy for moving fuel rods in water, which limits the maximum rod deflection during transference, resulting in minimal residual vibration of the rod at the target position within the nuclear reactor.

Fuel-rod vibration problems under the influence of hydrodynamic forces have been discussed in the literature; most works though have dealt with only the responses to the coolant flow (axial flow) after core insertion [4]–[6]. This study investigates the vibrational response of the fuel rod to the cross flows in the course of trolley movement. Recently, Shah and Hong have developed an input-shaping control method [7] under the pin-joint assumption between the trolley and the rod (i.e., the master fuel assembly). However, such assumption has turned out to be naive, because it does not account for the deflection of the rod itself. Therefore, in this paper, the fuel rod is regarded fixed to the trolley platform of the crane. Accordingly, the RM is considered as a hybrid system consisting of a lumped-mass trolley system and a flexible master fuel assembly system that exhibits transverse displacements in water.

The dynamics and control problems of flexible systems (in air) have been extensively studied over the past decades [8]–[14]. Particularly, the dynamics and control problems of a flexible inverted pendulum on a moving cart in air [13], [14] are closely related to the control problem of overhead cranes. However, control problems of moving objects in water are rare. Three essential differences between moving objects in air and those in water have been noted.

1) The natural frequency in water becomes different from that in air (i.e., in water, the effects of added mass and viscous damping must be considered).
2) From the command-shaping control viewpoint, the maximum speed of the trolley in air is restricted only by the length of the rod, whereas in water, it is restricted not only by the length but also by the deflection of the rod.
3) In water, the restriction on the maximum deflection of the rod becomes more important, whereas in air, the suppression of the rod's residual vibration is the top priority.

Several researchers have investigated the dynamics of flexible beams and cylinders in fluids (specifically in water) [15]–[22]. Han and Xu [16], Jones [17], and Xing *et al.* [18] individually reported vibration analyses of Euler–Bernoulli beams immersed in water, highlighting the effect of the surrounding fluid on the natural frequencies of the beams. In [19]–[22], the dynamics of deep-sea oil exploration systems were discussed in relation to the hydrodynamic force acting along the length of cantilever

Manuscript received November 29, 2016; revised April 3, 2017; accepted May 8, 2017. Date of publication May 19, 2017; date of current version August 14, 2017. Recommended by Technical Editor L. Zuo. This work was supported in part by the National Research Foundation of Korea under the Ministry of Science, ICT, and Future Planning, Korea, under Grant NRF-2014-R1A2A1A10049727, and in part by the Korea Institute of Marine Science and Technology Promotion under the Ministry of Oceans and Fisheries, Republic of Korea, under Grant 201309550001. *(Corresponding author: Keum-Shik Hong.)*

U. H. Shah and K.-S. Hong are with the School of Mechanical Engineering, Pusan National University, Busan 46241, South Korea (e-mail: umershah@pusan.ac.kr; kshong@pusan.ac.kr).

S.-H. Choi is with the Port Research Division, Korea Maritime Institute, Busan 49111, South Korea (e-mail: shchoi@kmi.re.kr).

Color versions of one or more of the figures in this paper are available online at http://ieeexplore.ieee.org.

Digital Object Identifier 10.1109/TMECH.2017.2706304

beam, one end of which was fixed to the seabed, the other was free having a tip mass (i.e., a ship/vessel to which a riser was attached). In most of these works, only the dynamics of the beam itself were considered. In this paper, the dynamics of the flexible rod (in water) as well as the trolley (in air) are considered in analyzing the underwater (UW) vibrational response of the rod.

For underactuated systems, various control techniques have been developed [23]–[50]. The crane is a typical underactuated system, and the sway suppression of the load can be achieved by implementing either open-loop control [34], [38]–[47] or feedback control, for instance, feedback linearization [30], sliding mode [31], [32], model predictive control [35], and Lyapunov function-based feedback control [36], [37].

Implementation of feedback control for a flexible rod in water is highly problematic owing to the difficulty of acquiring a proper sensor that functions well in water, besides the issue of distributed measurement. Also, attaching a sensor to the master fuel assembly requires an approval from the Nuclear Safety and Security Commission. Therefore, as an alternative method to feedback control, a command-shaping control [38], which is recognized as the most practical open-loop control technique for crane systems [42], [43], is considered in this paper for the suppression of the rod's residual vibrations in water. Our preliminary investigations, however, revealed that due to the presence of the hydrodynamic force, the existing command-shaping methods need to be modified for the systems in water. Therefore, a new shaping method satisfying the maximum deflection constraint during the trolley transference and the suppression of residual vibrations in water is developed. Earlier, Vossler and Singh [46] proposed a time-optimal control strategy for generating a shaped command that limits the maximum transient deflection of a flexible structure moving in air. In this paper, a similitude analysis is also performed in investigating the rod's deflection in water caused by the trolley input. Similitude analysis has been utilized in many engineering problems [51], [52] in predicting the behavior of the real system based on the behavior of a scaled model. A number of similitude methods are available for investigation of the structural vibrations of a nuclear power plant's components [53], [54]. The application of similitude analysis to the development of a control law for residual vibration suppression of a flexible rod in water, though, has not yet been reported.

In this paper, a distributed-parameter model of the RM is considered in investigating the UW transverse vibrations of the rod caused by trolley movement. The flexible rod exhibits a larger deflection in water than in air, whose deflection must be suppressed to ensure reactor safety. Using the results obtained thereby, an appropriate control law is formulated. A similitude analysis of the RM will reveal that, in water, the deflection variation of the rod is equal to the square of the velocity variation of the trolley, whereas, in air, a direct relationship exists between the rod's displacement and the trolley input. Therefore, the obtained similitude law relating the trolley velocity with the rod deflection together with the constraint on the maximum endpoint deflection of the rod is considered in developing a new command-shaping method for suppression of residual rod vibrations in water. The shaped command obtained through the newly proposed shaping technique consists, unlike the existing symmetric zero-vibration (ZV) and zero-vibration derivative (ZVD) shaped commands, of asymmetric acceleration and deceleration commands. Simulation and experimental results establish the newly proposed command's better residual vibration suppression performance for UW operations as compared with the existing methods.

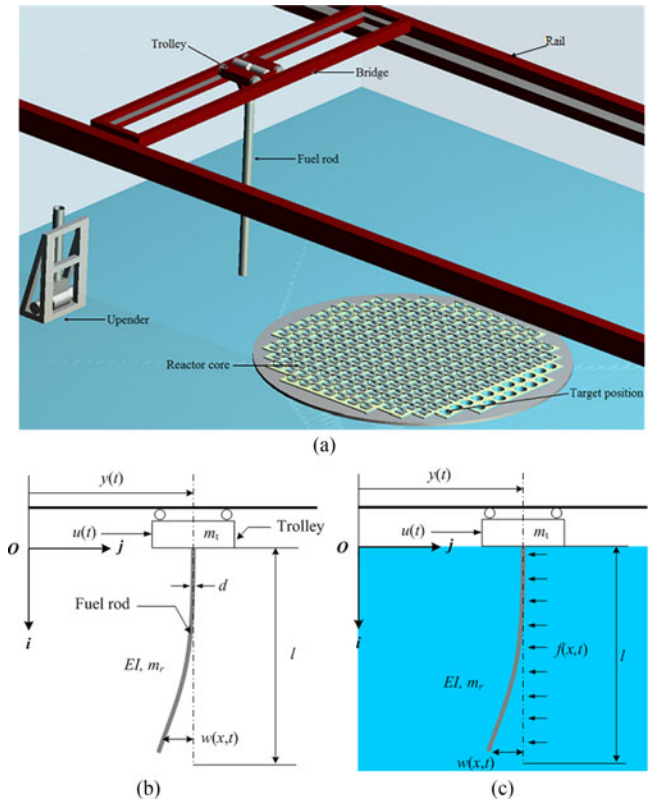

Fig. 1. RM: (a) three-dimensional schematic (see [7]); (b) 2-D schematic in air; and (c) 2-D schematic in water.

The main contributions of this paper include the investigation of the transverse displacement of a flexible rod in water in consideration of the dynamics of both the trolley and the rod, the development of a new command-shaping method in consideration of the maximum allowable rod deflection during trolley transference and the minimal residual vibrations, and the application of similitude analysis to the relation between the rod's deflection and the trolley velocity as it affects rod transportation in air and in water.

The rest of this paper is structured as follows. Section II discusses the dynamics of the hybrid system including the dynamics of a trolley and a flexible rod in water. Section III presents the system's response without any control, as obtained through simulations and experiments. Section IV explains the development of the proposed control technique. Finally, Section V analyzes the results obtained using the proposed control, and makes conclusions.

II. Problem Formulation

A. Equations of Motion

In Fig. 1, the master fuel assembly is assumed to be an Euler–Bernoulli beam with a circular cross section moving in water.

The trolley moves along the ***j***-axis. The friction between the trolley and the rails (in air) is assumed to be negligible. Let $y(t)$ be the trolley displacement along the ***j***-axis, $w(x, t)$ denote the transverse displacement of the rod at x and t, and m_t and m_r be the trolley mass and the rod mass, respectively. Let l, d, I, and E denote the length, the diameter, the area moment of inertia, and the Young's modulus of the rod, respectively, and $u(t)$ be the control input to the trolley.

For a rod moving in water, in Fig. 1(c), let $f(x, t)$ denote the nonconservative hydrodynamic force exerted on it by the surrounding water, which is given by the Morison equation [15] as follows:

$$f(x,t) = (\pi/4)\rho_w C_a(x) d^2 \dot{v}_r(x,t) + (1/2)\rho_w C_d(x) d v_r(x,t) \left|v_r(x,t)\right| \quad (1)$$

where C_a is the added-mass coefficient, C_d is the drag coefficient, and $v_r(x,t) = \dot{y}(t) + \dot{w}(x,t)$ is the velocity of the rod. By splitting $f(x, t)$ into two parts (inertial and drag components), (1) can be rewritten as

$$f(x,t) = f_m(x,t) + f_d(x,t) \quad (2)$$

where

$$f_m(x,t) = (\pi/4)\rho_w C_a(x) d^2 (\ddot{y}(t) + \ddot{w}(x,t))$$
$$f_d(x,t) = (1/2)\rho_w C_d(x) d (\dot{y}(t) + \dot{w}(x,t)) \left|\dot{y}(t) + \dot{w}(x,t)\right|.$$

Let c be the viscous damping coefficient in water. Then, the damping force in opposition to the motion of the rod is given by $-c\dot{w}(x,t)$ [20].

Using the Hamilton principle [55], the following equations of motion are now obtained:

$$(m_t + m_r)\ddot{y}(t) + m\int_0^l \ddot{w}(x,t)dx = u(t) \quad (3)$$

$$EIw''''(x,t) + c\dot{w}(x,t) + m\ddot{w}(x,t) = -m\ddot{y}(t) - f_d(x,t) \quad (4)$$

where $m = (m_r/l) + (\pi/4)\rho_w C_a(x) d^2$ is the (combined) mass per unit length of the rod and the fluid displaced by the rod. The derivatives with respect to t and x are denoted by $\dot{}$ and $'$, respectively. The boundary conditions are given as follows:

$$w(0,t) = 0,\ w'(0,t) = 0,\ w''(l,t) = 0, \text{and } w'''(l,t) = 0. \quad (5)$$

It is noted that, in comparison with the rod mounted on a moving cart in air [13], two new terms $c\dot{w}(x,t)$ and $f_d(x, t)$ appear in the model of a moving rod in water. Also, m in water includes the added fluid mass.

B. UW Response

The effect of trolley movement on the rod's response in water is to be analyzed. Substituting $\ddot{y}(t)$ from (3) into (4), the following equation representing the coupled dynamics of the trolley and the rod is obtained:

$$EIw''''(x,t) + c\dot{w}(x,t) + m\ddot{w}(x,t) = -\frac{m}{m_t + m_r}\left(u(t) - m\int_0^l \ddot{w}(x,t)dx\right) - f_d(x,t). \quad (6)$$

The preliminary investigation [7] revealed that the deflection of the rod is constant when the trolley moves at its constant maximum velocity $v_{\max}$. Also, a large trolley velocity causes a large rod deflection, which can damage the structure of the rod. Therefore, the relationship between the maximum rod deflection and the maximum trolley velocity has to be found. To get an analytic solution, the drag force term in (6) is approximated to $f_d(x,t) = (1/2)\rho_w C_d(x) d v_{\max} |v_{\max}|$, see [21] (or [22]).

1) Natural Frequencies and Normal Modes: The natural frequencies in water are different from those in air. Recall that c and f in (6) do not appear in air, and m also is different. However, the mode shapes are the same [17]. In this paper, the approach in [14] is adopted. Using the separation of variables, the mode shapes of the rod in water are obtained as follows:

$$\begin{aligned}\Phi_k(x) &= (C_k / \sin\beta_k l \sinh\beta_k l) \\ &\cdot ((1 + \cos\beta_k l \cosh\beta_k l)(2 - \cos\beta_k x - \cosh\beta_k x) \\ &+ (\cos\beta_k x - \cosh\beta_k x)(\sin\beta_k l \sinh\beta_k l) \\ &- (\cos\beta_k l \sinh\beta_k l + \sin\beta_k l \cosh\beta_k l)(\sin\beta_k x - \sinh\beta_k x))\end{aligned} \quad (7)$$

where k denotes an infinite number of modes, C_k are the arbitrary constants chosen for normalization purposes, and β_k are the solutions of the following frequency equation:

$$1 + \cos\beta_k l \cosh\beta_k l + (\cos\beta_k l \sinh\beta_k l + \sin\beta_k l \cosh\beta_k l)(r_m/\beta_k l) = 0 \quad (8)$$

where $r_m = m_r/m_t$ denotes the mass ratio of the rod to the trolley.

For the vibrating rod in water, the additional mass of the water displaced by the rod affects the natural frequencies. The obtained natural frequencies [16] are

$$\omega_{nk} = \frac{{\beta_k}^2 d}{4l^2}\sqrt{\frac{E}{\rho_r + C_a\rho_w}} \quad (9)$$

where ρ_r is the density of the rod, C_a is the added mass coefficient, and ρ_w is the density of water. In this paper, only the fundamental mode of the damped natural frequencies is considered (hereafter denoted by ω_1, i.e., $\omega_1 = \omega_{n1}$).

2) Time Response: The time response of the rod is obtained by applying the modal analysis method [55], which gives the following endpoint rod deflection;

$$w(l,t) = \frac{\Phi(l)}{\omega_d}\int_0^t Q(\tau)\, e^{-\zeta\omega_1(t-\tau)} \sin\omega_d(t-\tau)d\tau \quad (10)$$

where $\Phi(l) = \Phi_1(l)$, ζ denotes the damping ratio associated with the first mode, which can be obtained by comparing the experimental and simulation results of the system (see [7]), $\omega_d = \omega_1\sqrt{1-\zeta^2}$ is the first damped fundamental natural frequency of the rod, and $Q(t)$ is the generalized force acting on the system.

The steady-state endpoint deflection $w(l,t)_{ss} = \delta$ of the rod is required to be obtained when the trolley moves with a constant maximum velocity (i.e., $\dot{y}(t) = v_{\max}$). For the present case, the generalized force $Q(t)$ is given as follows:

$$Q(t) = -\Phi(l)\left(\pi\rho_w C_a(l)d^2\ddot{y}(t)/4 + \rho_w C_d(l)d\dot{y}^2(t)/2\right) - m\Phi(0)\ddot{y}(t). \tag{11}$$

Therefore, the endpoint displacement of the rod $w(l, t)$, when the trolley input $\ddot{y}(t)$ is considered as a pulse (i.e., magnitude a and interval t_a) is obtained as follows:

$$w(l,t) = -\frac{B_1}{\omega_d}\int_0^{t_a} e^{-\zeta\omega_1(t-\tau)}\sin\omega_d(t-\tau)d\tau - \frac{B_2}{\omega_d}\int_0^{t_a}\tau^2 e^{-\zeta\omega_1(t-\tau)}\sin\omega_d(t-\tau)d\tau - \frac{B_3}{\omega_d}\int_{t_a}^{t} e^{-\zeta\omega_1(t-\tau)}\sin\omega_d(t-\tau)d\tau \tag{12}$$

where $B_1 = \Phi(l)(m\Phi(0) + \Phi(l)f_m(l))a$, $B_2 = f_d(l)\Phi(l)^2 a$, and $B_3 = f_d(l)(\Phi(l)v_{\max})^2$. When the transient response dies out [the first two terms in (12)], the endpoint displacement in the steady state δ is obtained as follows:

$$\delta \triangleq w(l,t)_{ss} = -f_d(l)\left(\Phi(l)v_{\max}/\omega_1\right)^2. \tag{13}$$

Equation (13) will be used in developing the control law for transporting the flexible rod in water, while limiting its endpoint deflection and assuring the minimal residual vibration at the target position.

C. Similitude Analysis

In this section, to determine the relationship between the endpoint displacement of the rod in water and the maximum trolley velocity, a similitude law is formulated according to the Buckingham π theorem [51]. Using the fundamental dimensions (length L, mass M, time T), seven variables are selected: $\delta\,[L]$, $l\,[L]$, $\omega_1\,[T^{-1}]$, $d\,[L]$, $m_t\,[M]$, $u\,[MLT^{-2}]$, and $m_r\,[M]$. The similitude law for the considered problem is obtained (see [52] for details) as follows:

$$\frac{\delta}{l} = \varphi\left(r_a, r_m, \omega_1\sqrt{\frac{lm_r}{u}}\right) \tag{14}$$

where r_a denotes the aspect ratio (i.e., l/d) of the rod, u ($= u(t)$) is the control input to the trolley, and φ is the similitude function to be determined analytically. Let δ_m and δ_p be the steady-state deflections of the rod when u in (14) is given as u_m and u_p, respectively (either in the mathematical model or in the experiment). Because all of the parameters in (14) except u are fixed, the following similarity condition is obtained:

$$\delta_m/\delta_p = u_m/u_p. \tag{15}$$

If the relationship between δ and $v_{\max}$ in (13) is used, the similarity condition in water is represented by the equation

$$\delta_m/\delta_p = (v_{\max,m}/v_{\max,p})^2 \tag{16}$$

TABLE I
SIMULATION PARAMETERS

Parameters	Unit	Value
Rod length (l)	m	1.0
Rod diameter (d)	m	0.008
Rod mass (m_r)	kg	0.0369
Trolley mass (m_t)	kg	3.8011
Fundamental natural frequency (ω_1)	rad/s	9.52
Young's modulus (E)	GPa	3.89
Density of fuel rod (ρ_r)	kg/m^3	1204.5
Viscous damping coefficient (c)	N·s/m	0.6
Damping ratio (ζ)	–	0.56
Added-mass coefficient (C_a; see [16])	–	0.93
Drag coefficient (C_d; see [7])	–	1.28

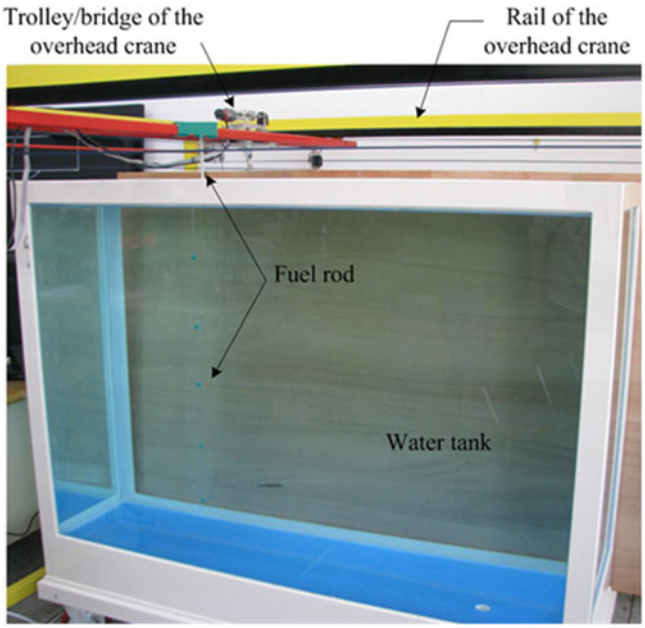

Fig. 2. Experimental setup.

where $v_{\max,m}$ and $v_{\max,p}$ denote the maximum trolley velocities associated with u_m and u_p, respectively. Similarity condition (16) signifies that a change (i.e., δ_m/δ_p) of the endpoint deflection in the steady state is equal to the square of the change of the maximum velocity of the trolley (i.e., $v^2_{\max,m}/v^2_{\max,p}$).

Remark: The similarity conditions in air (15) and that in water (16) are different. This difference must be incorporated into the design of an appropriate UW shaper (i.e., the maximum velocity of the trolley for UW maneuvering has to be carefully selected in consideration of the maximum allowable deflection of the rod).

III. SIMULATIONS AND EXPERIMENTATION

To figure out the rod deflection upon a trolley movement, (4) is first solved numerically by implementing the finite difference method (FDM). Simulations were performed using the parameters in Table I and MATLAB. The experimental setup consists of an Inteco 3-D Crane system combined with a water tank in which a flexible rod is transported by the crane's trolley. Fig. 2

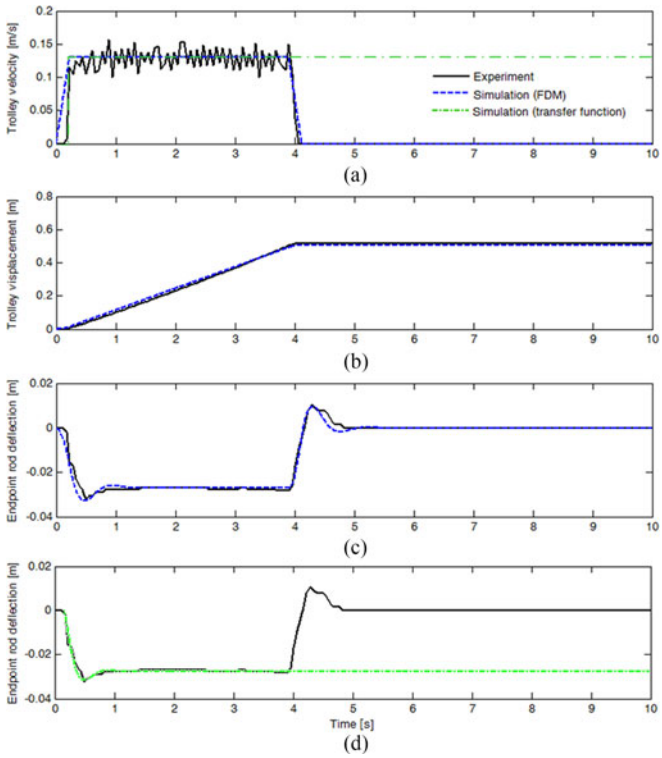

Fig. 3. Comparison of simulated and experimental results in water: (a) velocity commands; (b) trolley displacements; (c) experimental and simulation (FDM) responses; and (d) experimental and simulation (transfer function) responses.

shows the experimental setup. A comparison of the simulated and experimental rod responses to a reference trolley velocity profile, shown in Fig. 3(a), is presented in Fig. 3(c). It can be seen in Fig. 3(c) that both simulated (dashed line) and experimental (solid line) rod responses match very well, which validate that the developed mathematical model of the UW system is correct.

Fig. 4 shows simulated endpoint displacements of the rod in air and in water for two different trolley inputs, where the rationale for having two inputs was to use them to illustrate the correctness of the similitude laws in (15) and (16). Fig. 4(a) depicts the two acceleration inputs to the trolley (i.e., $\ddot{y}_p = 1$ m/s^2 and $\ddot{y}_m = 1.5$ m/s^2), according to which the trolley was accelerated during the initial 0.2 s and decelerated during the last 0.2 s. Fig. 4(b) shows the two velocity profiles generated for the trolley (one having the maximum velocity at 0.2 m/s and the other at 0.3 m/s). The time taken by the trolley to reach the target position is indicated. Fig. 4(c) shows the trolley displacements (1.2 m) obtained by the given profiles. It can be seen that if $v_{\max}$ is high, the time taken to reach the target position is short. The endpoint displacements of the rod in air for the given profiles are presented in Fig. 4(d), and those in water, in Fig. 4(e).

As illustrated in Fig. 4(d), the amplitude of the endpoint displacement in air when $v_{\max,m} = 0.3\,\mathrm{m/s}$ (during the maximum velocity interval) is 0.02 m (say, δ_m), and that when $v_{\max,p} = 0.2$ m/s is 0.013 m (say, δ_p). Then, the ratio of the two amplitudes becomes $\delta_m/\delta_p = 1.53$. On the other hand, noting that $\ddot{y}_m = v_{\max,m}/t_m$ and $\ddot{y}_p = v_{\max,p}/t_p$, the two maximum velocities of the trolley result in $\ddot{y}_m/\ddot{y}_p = v_{\max,m}/v_{\max,p} = 1.5$, because the two acceleration intervals are the same (i.e., $t_m = t_p = 0.2\,\mathrm{s}$). Therefore, the similitude law in (15) in air is verified.

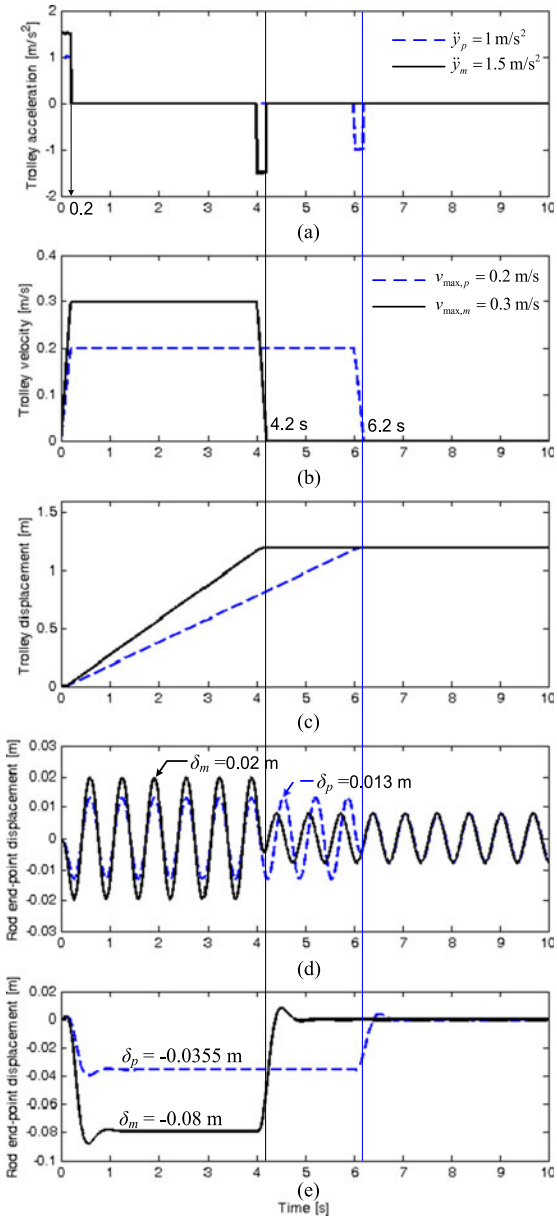

Fig. 4. Validation of similitude law (14) via two different trolley inputs: (a) trolley acceleration inputs; (b) trolley velocity profiles; (c) trolley displacements; (d) endpoint deflections in air; and (e) endpoint displacements in water.

In Fig. 4(e), the ratio of the maximum displacements in water is $\delta_m/\delta_p = 2.25$ (i.e., 0.08/0.0355). Also, $v^2_{\max,m}/v^2_{\max,p} = 0.3^2/0.2^2 = 2.25$. This means that the similitude law in water (16) is satisfied as well. In summary, the similitude analysis verified that the steady-state deflection in water is proportional to the square of the trolley velocity.

IV. Control Formulation and Implementation

This section discusses the control law derivation and its implementation for suppressing the fuel rod's residual vibrations in water. In a nuclear reactor, such external disturbances like

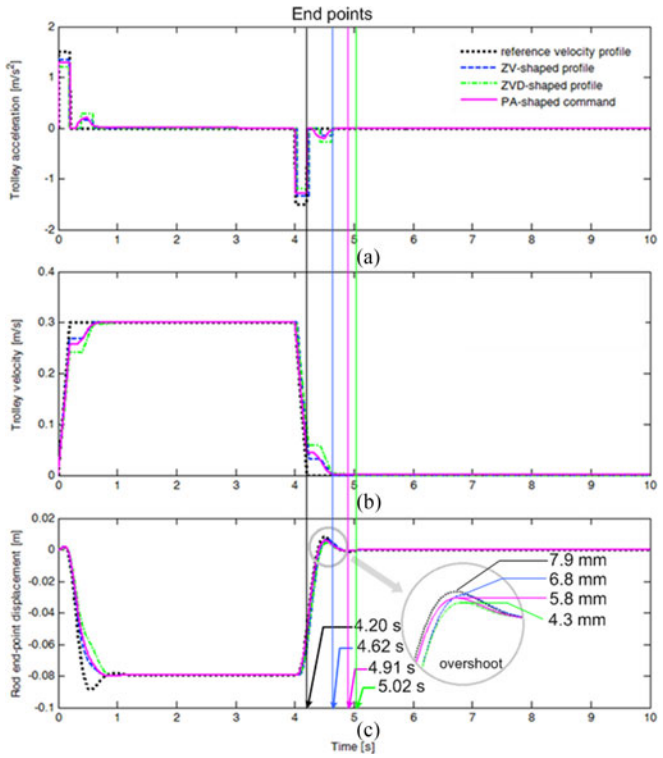

Fig. 5. UW responses of ZV, ZVD, and PA commands: (a) acceleration inputs; (b) velocity commands; and (c) endpoint deflections.

winds can be ignored. Also, as a fault-tolerant secondary control strategy backing up the primary feedback control, an open-loop control (a modified input shaping) is discussed in this paper. In implementing the input shaping control, a reference trolley-drive command is convolved with an input shaper for generating a shaped trolley velocity command. Then, the trolley controller makes the trolley to follow the generated shaped command, using the built-in velocity tracking algorithm [44], [45], which results in transporting the load to the target position with zero or minimal residual vibrations.

A. Command Shapers in Air

To examine whether the existing input-shaping methods in air work for the system in water or not, two input-shaped commands ZV and ZVD [38] were generated using the fundamental natural frequency of the system in water (i.e., ω_d). The target position was set to 1.2 m along the $\boldsymbol{j}$-axis. The maximum trolley acceleration $a_{\max}$ was 1.5 m/s^2. Fig. 5(b) plots the reference velocity profile (dotted line), the ZV-shaped command (dashed line), and the ZVD-shaped command (dash-dot line) for driving the trolley to the target position. In this study, the ZV-shaped command was obtained by convolving the reference velocity profile with the ZV shaper [38] as follows:

$$\begin{bmatrix} A_i \\ t_i \end{bmatrix} = \begin{bmatrix} \frac{1}{1+K} & \frac{K}{1+K} \\ 0 & \frac{\pi}{\omega_d} \end{bmatrix} = \begin{bmatrix} 0.9 & 0.1 \\ 0 & 0.4 \end{bmatrix} \tag{17}$$

where $K = e^{-\zeta\pi/\sqrt{1-\zeta^2}}$ (in our case, $\zeta = 0.56$, $K = 0.12$), i corresponds to the number of impulses, and A_i and t_i represent the magnitudes and time locations, respectively, of the impulses. Similarly, the ZVD-shaped command was obtained by convolving the reference velocity profile with the ZVD shaper [38] as follows:

$$\begin{bmatrix} A_i \\ t_i \end{bmatrix} = \begin{bmatrix} \frac{1}{(1+K)^2} & \frac{2K}{(1+K)^2} & \frac{K^2}{(1+K)^2} \\ 0 & \frac{\pi}{\omega_d} & \frac{2\pi}{\omega_d} \end{bmatrix} = \begin{bmatrix} 0.8 & 0.19 & 0.01 \\ 0 & 0.4 & 0.8 \end{bmatrix}. \tag{18}$$

As seen in Fig. 5(c), even by considering the natural frequency and the damping ratio of the UW system, the desired control performance (i.e., suppression of the rod's overshoot at a target position) was not achieved by implementing the ZV and the ZVD shapers (17), (18) [see Fig. 7(c) for comparison]. According to [47], an overshoot can be suppressed by considering the plant zeros in designing the shapers (i.e., a postactuation (PA) shaper). However, the plant zeros in our case cannot be obtained analytically, [56], [57], because of the nonlinear drag force term in (6). Therefore, the linear dynamics is approximately obtained experimentally by comparing the step response to a constant trolley input with a general second-order equation. Fig. 3(d) shows the experimental trolley response (solid line, black) and the simulated step response of the obtained second-order equation (dash-dot line, green), where their inputs are shown in Fig. 3(a).

Finally, for $\zeta = 0.56$ and $\omega_1 = 9.52$ rad/s, the following linear dynamics $G(s)_p$ (transfer function) is utilized:

$$G(s)_p = \frac{b_1 s^2 + b_2 s + b_3}{s^2 + 2\xi\omega_1 s + \omega_1^2} = \frac{0.1s + 2.5}{s^2 + 10.66s + 90.63} \tag{19}$$

which reveals one zero of the system (i.e., $s = -25$). Considering the method in [47], the following transfer function $G(s)_s$ of the PA shaper is obtained:

$$G(s)_s = 0.88 + 2.94\frac{e^{-0.35s}}{s + 25}. \tag{20}$$

Fig. 5 shows a comparison of the system response to the PA-shaped command (solid line) with the ZV- and ZVD-shaped commands. It can be seen in Fig. 5(c) that the PA-shaped command has reduced the overshoot as compared with the ZV shaper. However, the desired suppression of the overshoot has not been achieved. Therefore, for vibration suppression of the rod in water, a new means of obtaining the shaped trolley command for complete suppression of the overshoot at the target position is absolutely necessary.

B. UW Command Shaping

The existing input-shaping methods utilize two or more pulses in that the resulting transient motion of the system cancels each other to achieve zero (or minimal) residual vibration. However, application of pulses in water results not in cancellation of the

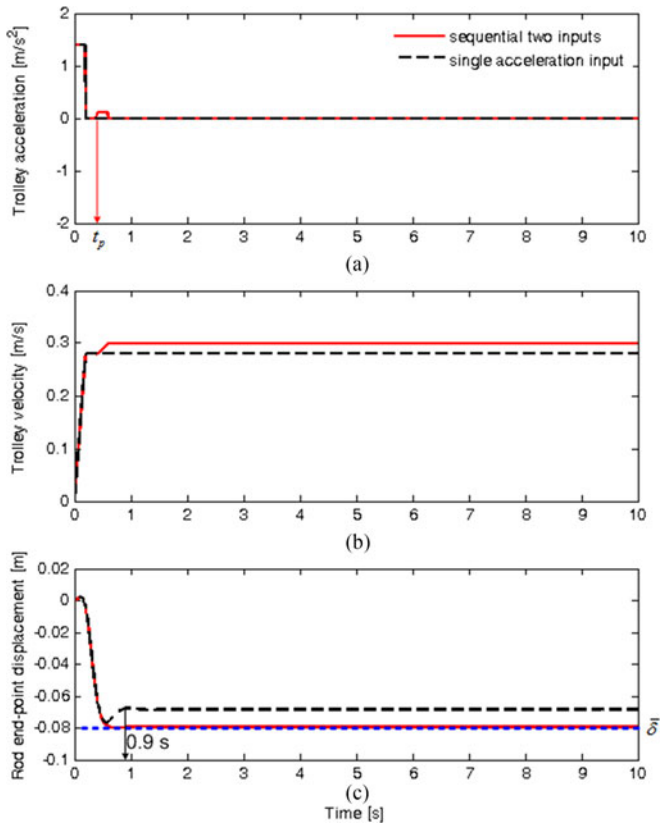

Fig. 6. Concept of UW command shaping: (a) acceleration inputs; (b) velocity commands; and (c) endpoint deflections.

transient response but rather in its amplification due to hydrodynamic force. Hence, this paper's proposed new shaping method is based on an amplification of the rod's response to a trolley input.

In order to avoid structural damage incurred to a fuel rod transported in water, it is imperative to restrict the magnitude of the input to the trolley to ensure that the maximum endpoint deflection of the rod is less than a specified maximum allowable value ($\bar{\delta}$). Application of an acceleration input (pulse) to the trolley [the dashed line in Fig. 6(a)] results in a maximum rod overshoot ($\max|w(l,t)|$) that is equal to $\bar{\delta}$ [the dotted blue line in Fig. 6(c)]. Fig. 6(c) demonstrates that when the trolley is driven by that input, the rod achieves the steady-state deflection (δ) at 0.9 s. It is anticipated that if the magnitude of the input is increased in such a way that $\delta = \bar{\delta}$, the time taken by the trolley to reach the target position can be reduced. However, an increase in input magnitude will cause $\max|w(l,t)|$ to exceed $\bar{\delta}$, because for a given acceleration (input) interval, the higher the $v_{\max}$ is, the larger the $\max|w(l,t)|$ and the δ will be [see Fig. 4(e)], though the time to the maximum overshoot is the same (i.e., the peak time $t_{\text{peak}} = \pi/\omega_d$ is the same). Therefore, two sequential inputs (the same interval, different magnitudes), shown by the solid line in Fig. 6(a), are applied to achieve the steady-state response with zero oscillation [i.e., the rod reaches the steady state without overshoot; see Fig. 6(c)]. This is achieved by applying the second input at the time of the occurrence of the overshoot of the first input, provided that the magnitude of the second input is selected in such a way that the resulting steady-state deflection of the rod equals the maximum (or minimum) rod deflection due to the first input. Furthermore, the acceleration and deceleration inputs obtained from the proposed UW-command-shaping method are asymmetric, unlike the symmetric ZV and ZVD commands. Similar multiple-pulse-based control approaches [58]–[60] have been reported in the literature for moving flexible systems in air under the influence of friction.

1) Acceleration Inputs: Similarity condition (16) and the following constraint on the maximum endpoint displacement of the rod are used in formulating the magnitudes of two acceleration inputs:

$$\max|w(l,t)| = |\delta|\ (1\ +\ K)\ \le\ \left|\bar{\delta}\right| \tag{21}$$

where $\bar{\delta}$ denotes the maximum allowable value for the endpoint deflection of the rod. Now, let δ_1 denotes the steady-state deflection of the rod caused by the maximum trolley velocity $v_{\max,1}$ (associated with the first input a_1). Substituting (21) into (13) yields

$$v_{\max,1} = \frac{\omega_1}{\Phi(l)}\sqrt{\frac{|\delta_1|}{f_d}} = \frac{\omega_1}{\Phi(l)}\sqrt{\frac{|\bar{\delta}|}{f_d(1+K)}}. \tag{22}$$

Accordingly, the magnitude of the first input can be obtained as follows:

$$a_1 = \frac{v_{\max,1}}{t_a} = a_{\max}\sqrt{\frac{1}{1\ +\ K}} \tag{23}$$

where $t_a = v_{\max}/a_{\max}$, and $a_{\max}$ is the given allowable maximum acceleration to the trolley system. If $\bar{\delta}$ is the resultant steady-state deflection of the rod due to two acceleration inputs, the maximum trolley velocity can be obtained from (13) as follows:

$$v_{\max} = \frac{\omega_1}{\Phi(l)}\sqrt{\frac{|\bar{\delta}|}{f_d}}. \tag{24}$$

Now, by application of similarity condition (16), the maximum trolley velocity corresponding to the second input $v_{\max,2}$ can be obtained as follows:

$$v_{\max,2} = v_{\max,1}\left(\sqrt{\left|\frac{\bar{\delta}}{\delta_1}\right|} - 1\right) = v_{\max,1}\left(\sqrt{1\ +\ K} - 1\right). \tag{25}$$

Therefore, the magnitude of the second acceleration input becomes

$$a_2 = \frac{v_{\max,2}}{t_a} = a_{\max}\left(1 - \sqrt{\frac{1}{1\ +\ K}}\right). \tag{26}$$

2) Deceleration Inputs: In order to obtain the magnitudes of the deceleration inputs, deflection constraint (21) is written in the following form:

$$\left|\bar{\delta}\right| K - |\delta|\,(1\ +\ K) = 0. \tag{27}$$

Now, let δ_3 denote the steady-state deflection of the rod caused by the maximum trolley velocity $v_{\max,3}$ (associated with the first

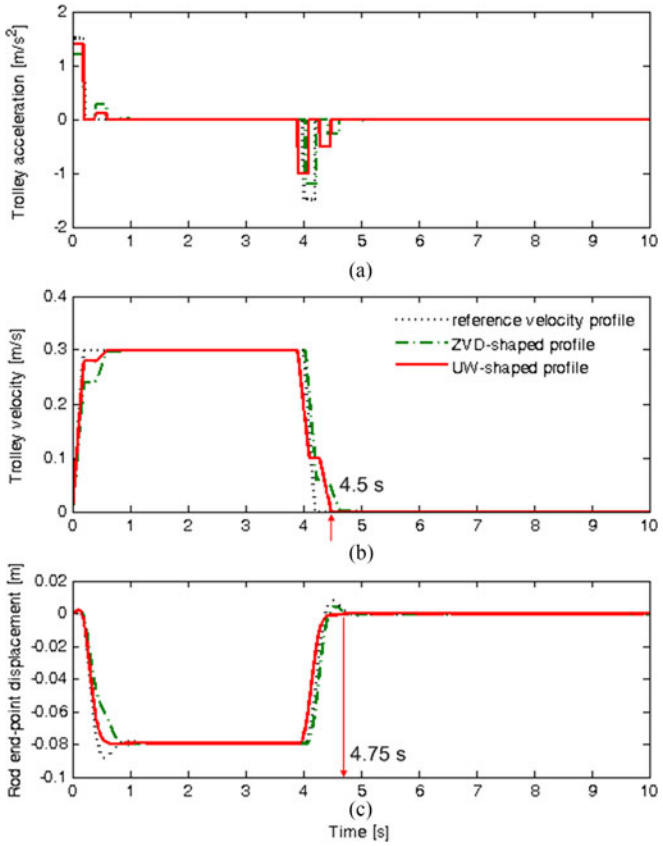

Fig. 7. UW responses of the proposed UW command: (a) acceleration inputs; (b) shaped velocity commands; and (c) endpoint deflections.

deceleration input a_3). Substituting (27) into (13) yields

$$v_{\max,3} = v_{\max} - \frac{\omega_1}{\Phi(l)}\sqrt{\frac{|\bar{\delta}|}{f_d}}\frac{K}{1+K}. \tag{28}$$

Accordingly, the magnitude of the first deceleration input a_3 can be obtained as follows:

$$a_3 = \frac{v_{\max,3}}{t_a} = a_{\max}\left(1 - \sqrt{\frac{K}{1+K}}\right). \tag{29}$$

The trolley velocity corresponding to the second input $v_{\max,4}$ can be obtained from similarity condition (16) as $v_{\max,4} = v_{\max} - v_{\max,3}$. This results in the following magnitude of the second deceleration input:

$$a_4 = \frac{v_{\max,4}}{t_a} = \sqrt{\frac{K}{1+K}}. \tag{30}$$

In light of the foregoing discussion, the UW shapers for obtaining the acceleration and deceleration inputs can be summarized as follows.

1) UW shaper for acceleration inputs

$$\begin{bmatrix} A_i \\ t_i \end{bmatrix} = \begin{bmatrix} \sqrt{\frac{1}{1+K}} & 1 - \sqrt{\frac{1}{1+K}} \\ 0 & \frac{\pi}{\omega_d} \end{bmatrix}. \tag{31}$$

TABLE II
COMPARISON OF RESPONSES FOR VARIOUS SHAPED COMMANDS

Trolley-drive command	Travel Time [s]	Settling time [s]	Maximum overshoot [mm]	Overshoot suppression [%]
Reference command (Trapezoidal)	4.20	5.205	7.9	–
ZV-shaped command	4.62	5.175	6.8	14%
PA-shaped command	4.91	5.12	5.8	25.3%
ZVD-shaped command	5.02	5.155	4.3	45.5%
UW-shaped command (the proposed one)	4.50	4.75	0.1	98.7%

2) UW shaper for deceleration inputs

$$\begin{bmatrix} A_i \\ t_i \end{bmatrix} = \begin{bmatrix} 1 - \sqrt{\frac{K}{1+K}} & \sqrt{\frac{K}{1+K}} \\ t_3 & t_3 + \frac{\pi}{\omega_d} \end{bmatrix} \tag{32}$$

where t_3 is the time of application of the first deceleration input. Finally, (31), (32) can be utilized to generate the following shaped acceleration command to drive the trolley to the target position in time $t_f = t_3 + t_a + \pi/\omega_d$:

$$\ddot{y}(t) = \begin{cases} a_{\max}\sqrt{\frac{1}{1+K}}, & \text{for } 0 \le t \le t_a \\ a_{\max}\left(1 - \sqrt{\frac{1}{1+K}}\right), & \text{for } \frac{\pi}{\omega_d} \le t \le t_a + \frac{\pi}{\omega_d} \\ -a_{\max}\left(1 - \sqrt{\frac{K}{1+K}}\right), & \text{for } t_3 \le t \le t_3 + t_a \\ -a_{\max}\sqrt{\frac{K}{1+K}}, & \text{for } t_3 + \frac{\pi}{\omega_d} \le t \le t_f \\ 0, & \text{otherwise.} \end{cases} \tag{33}$$

The generated control command is obtained based on the system's natural frequency and damping ratio. Therefore, its implementation for the actual system requires only simple computations of (31), (32) and prior knowledge of the system's natural frequency and damping ratio.

Fig. 7 compares the residual vibration suppression performance of the UW-shaped command with that of the ZVD-shaped command. Fig. 7(a) shows the reference acceleration command (dotted line), the ZVD-shaped command (dash-dot line), and the UW-shaped command (solid line). The applied $\bar{\delta}$ and $a_{\max}$ values were 0.08 m and 1.5 m/s^2, respectively. The velocity profiles corresponding to the given acceleration inputs are plotted in Fig. 7(b). It is apparent that when driven by the UW-shaped velocity profile, the trolley reaches the target position in 4.5 s. Fig. 7(c), meanwhile, shows, again with the UW-shaped velocity profile, that the settling time of the residual vibrations of the rod is 4.75 s. Thus, it is demonstrated that the proposed shaped command (33), as compared with the existing input-shaped commands, effectively suppresses the overshoot in the rod's response when transported in water. A comparison of the rod's responses for all of the considered profiles is shown in Table II.

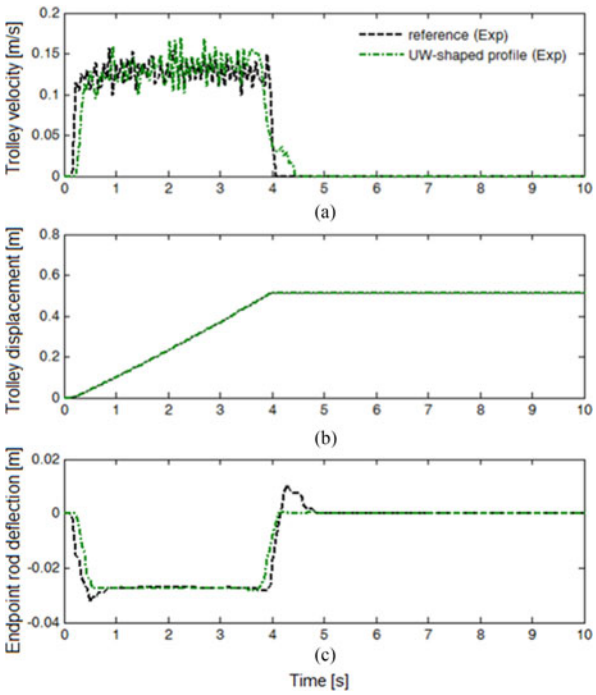

Fig. 8. Experimental results in water to the reference and UW-shaped commands: (a) velocity commands; (b) trolley displacements; and (c) endpoint deflections.

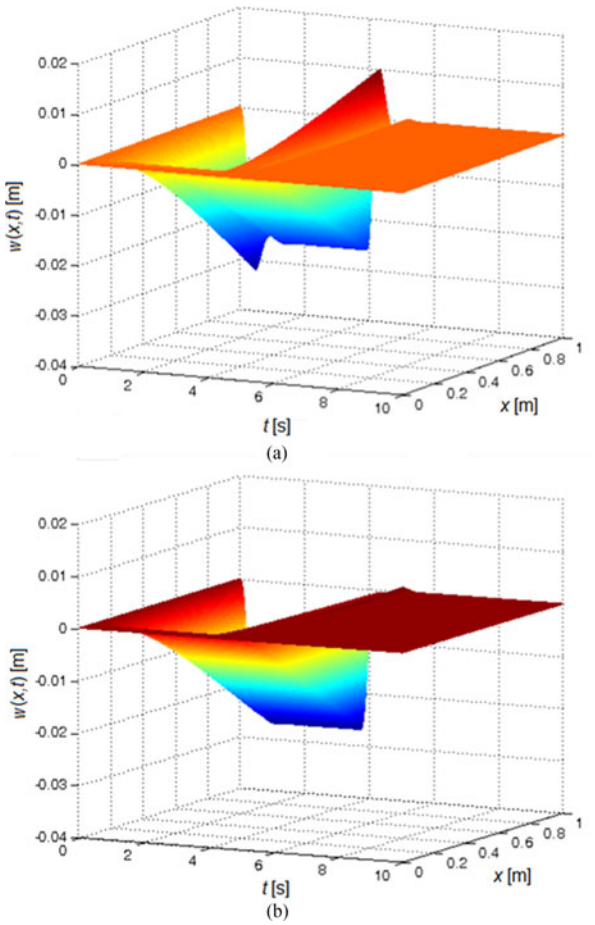

Fig. 9. Three-dimensional plots of rod deflections in water: (a) without control; and (b) with UW-command-shaping control.

V. Results and Conclusion

The data on the UW responses of the fuel rod for all the considered trolley inputs (i.e., the reference command, the ZV command, the ZVD command, the PA command, and the UW-shaped command) established the utility of our method [see Fig. 7(c) and Table II]. The UW-shaped command took the shortest time (i.e., 4.5 s) in transporting the fuel rod to the target position in water while successfully suppressing its residual vibrations. Moreover, it reduced the settling time by 10%. Overall, the newly proposed UW-command-shaping method, as specifically designed for suppression of the residual vibrations of flexible loads in water, outperforms the existing ZV, ZVD, and PA velocity profiles. To validate the developed control scheme, experiments were performed. Videos of the experiments were also provided. Fig. 8(c) presents a comparison of the experimental rod responses to the reference and UW-shaped trolley velocity commands. Furthermore, Fig. 9(a) and (b) depicts simulated 3-D plots of the rod deflection in water to the reference and UW-shaped trolley velocity commands.

In summary, this study, for a nuclear-reactor RM, developed a distributed-parameter model representing the response of a nuclear-fuel rod to its transportation in water. A new UW-command-shaping method was developed in consideration of the hydrodynamic force acting on the rod. A similitude law relating the rod's deflection in water to the trolley input, together with a constraint for the maximum endpoint deflection of the rod, was used to obtain the shaped velocity profiles. The simulation and experimental results reveal that our proposed method is, as compared with the existing input shapers, the most suitable for suppression of the residual vibrations of flexible systems operating in water.

References

[1] S.-S. Lee, S.-H. Kim, and K.-Y. Suh, "The design features of the advanced power reactor 1400," *Nucl. Eng. Technol.*, vol. 41, no. 8, pp. 995–1004, Oct. 2009.

[2] K.-T. Kim, "A study on the grid-to-rod fretting wear-induced fuel failure observed in the 16 × 16 KOFA fuel," *Nucl. Eng. Des.*, vol. 240, no. 4, pp. 756–762, Apr. 2010.

[3] *Design of Fuel Handling and Storage Systems for Nuclear Power Plants*, International Atomic Energy Agency, Vienna, Austria, Safety Standards Series No. NS-G-1.4, Aug. 2003.

[4] R. T. Pavlica and R. C. Marshall, "An experimental study of fuel assembly vibrations induced by coolant flow," *Nucl. Eng. Des.*, vol. 4, no. 1, pp. 54–60, May 1966.

[5] D. Basile, J. Faure, and E. Ohlmer, "Experimental study on the vibrations of various fuel rods in parallel flow," *Nucl. Eng. Des.*, vol. 7, no. 6, pp. 517–534, Jun. 1968.

[6] S. S. Chen, "Vibration of nuclear fuel bundles," *Nucl. Eng. Des.*, vol. 35, no. 3, pp. 399–422, 1975.

[7] U. H. Shah and K.-S. Hong, "Input shaping control of a nuclear power plant's fuel transport system," *Nonlinear Dyn.*, vol. 77, no. 4, pp. 1737–1748, Sep. 2014.

[8] E. Barbieri and U. Ozguner, "Unconstrained and constrained mode expansions for a flexible slewing link," *J. Dyn. Syst. Meas. Control, Trans. ASME*, vol. 110, no. 4, pp. 416–421, Dec. 1988.

[9] J. A. Mynderse and G. T. C. Chiu, "Two-degree-of-freedom hysteresis compensation for a dynamic mirror actuator," *IEEE/ASME Trans. Mechatronics*, vol. 21, no. 1, pp. 29–37, Feb. 2016.

[10] X. Wang, H. Gao, O. Kaynak, and W. Sun, "Online deflection estimation of X-axis beam on positioning machine," *IEEE/ASME Trans. Mechatronics*, vol. 21, no. 1, pp. 339–350, Feb. 2016.

[11] B. Xiao, S. Yin, and O. Kaynak, "Attitude stabilization control of flexible satellites with high accuracy: An estimator-based approach," *IEEE/ASME Trans. Mechatronics*, vol. 22, no. 1, pp. 349–358, Feb. 2017.

[12] K.-J. Yang, K.-S. Hong, and F. Matsuno, "Robust adaptive boundary control of an axially moving string under a spatiotemporally varying tension," *J. Sound Vibr.*, vol. 273, nos. 4/5, pp. 1007–1029, Jun. 2004.

[13] J. Lin and W. S. Chao, "Vibration suppression control of beam-cart system with piezoelectric transducers by decomposed parallel adaptive neuro-fuzzy control," *J. Vibr. Control*, vol. 15, no. 12, pp. 1885–1906, Dec. 2009.

[14] S. Park, W. K. Chung, Y. Youm, and J. W. Lee, "Natural frequencies and open-loop responses of an elastic beam fixed on a moving cart and carrying an intermediate lumped mass," *J. Sound Vibr.*, vol. 230, no. 3, pp. 591–615, Feb. 2000.

[15] A. W. Troesch and S. K. Kim, "Hydrodynamic forces acting on cylinders oscillating at small amplitudes," *J. Fluids Struct.*, vol. 5, no. 1, pp. 113–126, Jan. 1991.

[16] R. P. S. Han and H. Z. Xu, "A simple and accurate added mass model for hydrodynamic fluid-structure interaction analysis," *J. Franklin Inst.*, vol. 333B, no. 6, pp. 929–945, Nov. 1996.

[17] A. T. Jones, "Vibrations of beams immersed in a liquid," *Exp. Mech.*, vol. 10, no. 2, pp. 84–88, 1970.

[18] J. T. Xing, W. G. Price, M. J. Pomfret, and L. H. Yam, "Natural vibration of a beam-water interaction system," *J. Sound Vibr.*, vol. 199, no. 3, pp. 491–512, Jan. 1997.

[19] S. K. Chakrabarti and R. E. Frampton, "Review of riser analysis techniques," *Appl. Ocean Res.*, vol. 4, no. 2, pp. 73–90, 1982.

[20] W. He, S. S. Ge, B. V. E. How, Y. S. Choo, and K.-S. Hong, "Robust adaptive boundary control of a flexible marine riser with vessel dynamics," *Automatica*, vol. 47, no. 4, pp. 722–732, Apr. 2011.

[21] R. D. Young, J. R. Fowler, E. A. Fisher, and R. R. Luke, "Dynamic analysis as an aid to the design of marine risers," *J. Pressure Vessel Technol., Trans. ASME*, vol. 100, pp. 200–205, 1978.

[22] G. K. Furnes, "On marine riser responses in time- and depth-dependent flows," *J. Fluids Struct.*, vol. 14, no. 2, pp. 257–273, Feb. 2000.

[23] K.-S. Hong and J. Bentsman, "Direct adaptive control of parabolic systems: Algorithm synthesis, and convergence and stability analysis," *IEEE Trans. Autom. Control*, vol. 39, no. 10, pp. 2018–2033, Oct. 1994.

[24] K.-S. Hong, H. C. Sohn, and J. K. Hedrick, "Modified skyhook control of semi-active suspensions: A new model, gain scheduling, and hardware-in-the-loop tuning," *J. Dyn. Syst. Meas. Control, Trans. ASME*, vol. 124, no. 1, pp. 158–167, Mar. 2002.

[25] W. Sun, H. Gao, and O. Kaynak, "Vibration isolation for active suspensions with performance constraints and actuator saturation," *IEEE/ASME Trans. Mechatronics*, vol. 20, no. 2, pp. 675–683, Apr. 2015.

[26] B. Yao, F. P. Bu, J. Reedy, and G. T. C. Chiu, "Adaptive robust motion control of single-rod hydraulic actuators: Theory and experiments," *IEEE/ASME Trans. Mechatronics*, vol. 5, no. 1, pp. 79–91, Mar. 2000.

[27] M. A. Khanesar, Y. Oniz, O. Kaynak, and H. Gao, "Direct model reference adaptive fuzzy control of networked SISO nonlinear systems," *IEEE/ASME Trans. Mechatronics*, vol. 21, no. 1, pp. 205–213, Feb. 2016.

[28] E. Kayacan, E. Kayacan, H. Ramon, and O. Kaynak, "Towards agrobots: Trajectory control of an autonomous tractor using type-2 fuzzy logic controllers," *IEEE/ASME Trans. Mechatronics*, vol. 20, no. 1, pp. 287–298, Feb. 2015.

[29] Q. C. Nguyen and K.-S. Hong, "Transverse vibration control of axially moving membranes by regulation of axial velocity," *IEEE Trans. Control Syst. Technol.*, vol. 20, no. 4, pp. 1124–1131, Jul. 2012.

[30] H. Park, D. Chwa, and K.-S. Hong, "A feedback linearization control of container cranes: Varying rope length," *Int. J. Control Autom. Syst.*, vol. 5, no. 4, pp. 379–387, Aug. 2007.

[31] Q. H. Ngo and K.-S. Hong, "Adaptive sliding mode control of container cranes," *IET Control Theory Appl.*, vol. 6, no. 5, pp. 662–668, Mar. 2012.

[32] Q. H. Ngo and K.-S. Hong, "Sliding-mode antisway control of an offshore container crane," *IEEE/ASME Trans. Mechatronics*, vol. 17, no. 2, pp. 201–209, Apr. 2012.

[33] J. Smoczek and J. Szpytko, "Particle swarm optimization-based multivariable generalized predictive control for an overhead crane," *IEEE/ASME Trans. Mechatronics*, vol. 22, no. 1, pp. 258–268, Feb. 2017.

[34] Z. Wu and X. Xia, "Optimal motion planning for overhead cranes," *IET Control Theory Appl.*, vol. 8, no. 17, pp. 1833–1842, Nov. 2014.

[35] Z. Wu, X. Xia, and B. Zhu, "Model predictive control for improving operational efficiency of overhead cranes," *Nonlinear Dyn.*, vol. 79, no. 4, pp. 2639–2657, Mar. 2015.

[36] N. Sun, Y. Wu, Y. Fang, and H. Chen, "Nonlinear stabilization control of multiple-RTAC systems subject to amplitude-restricted actuating torques using only angular position feedback," *IEEE Trans. Ind. Electron.*, vol. 64, no. 4, pp. 3084–3094, Apr. 2017.

[37] N. Sun, Y. Fang, H. Chen, and B. Lu, "Amplitude-saturated nonlinear output feedback antiswing control for underactuated cranes with double-pendulum cargo dynamics," *IEEE Trans. Ind. Electron.*, vol. 64, no. 3, pp. 2135–2146, Mar. 2017.

[38] W. Singhose, "Command shaping for flexible systems: A review of the first 50 years," *Int. J. Prec. Eng. Manuf.*, vol. 10, no. 4, pp. 153–168, Oct. 2009.

[39] J. Fortgang and W. Singhose, "Concurrent design of vibration absorbers and input shapers," *J. Dyn. Syst. Meas. Control, Trans. ASME*, vol. 127, no. 3, pp. 329–335, Sep. 2005.

[40] W. Chatlatanagulchai, D. Kijdech, T. Benjalersyarnon, and S. Damyot, "Quantitative feedback input shaping for flexible-joint robot manipulator," *J. Dyn. Syst. Meas. Control, Trans. ASME*, vol. 138, no. 6, pp. 061006-1—061006-13, Jun. 2016.

[41] R. Mar, A. Goyal, V. Nguyen, T. Yang, and W. Singhose, "Combined input shaping and feedback control for double-pendulum systems," *Mech. Syst. Signal Process.*, vol. 85, pp. 267–277, 2017.

[42] Z. N. Masoud and M. F. Daqaq, "A graphical approach to input-shaping control design for container cranes with hoist," *IEEE Trans. Control Syst. Technol.*, vol. 14, no. 6, pp. 1070–1077, Nov. 2006.

[43] M. F. Daqaq and Z. N. Masoud, "Nonlinear input-shaping controller for quay-side container cranes," *Nonlinear Dyn.*, vol. 45, nos. 1/2, pp. 149–170, Jul. 2006.

[44] A. Kamel, F. Lange, and G. Hirzinger, "New aspects of input shaping control to damp oscillations of a compliant force sensor," in *Proc. IEEE Int. Conf. Robot. Autom.*, May 2008, pp. 2629–2635.

[45] D.-W. Peng, T. Singh, and M. Milano, "Zero-phase velocity tracking of vibratory systems," *Control Eng. Pract.*, vol. 40, pp. 93–101, Jul. 2015.

[46] M. Vossler and T. Singh, "Minimax state/residual-energy constrained shapers for flexible structures: Linear programming approach," *J. Dyn. Syst. Meas. Control, Trans. ASME*, vol. 132, no. 3, pp. 031010-1–031010-8, May 2010.

[47] T. Singh, "Pole-zero, zero-pole cancelling input shapers," *J. Dyn. Syst. Meas. Control, Trans. ASME*, vol. 134, no. 1, pp. 011015-1—011015-10, Jan. 2012.

[48] K.-J. Yang, K.-S. Hong, and F. Matsuno, "Boundary control of a translating tensioned beam with varying speed," *IEEE/ASME Trans. Mechatronics*, vol. 10, no. 5, pp. 594–597, Oct. 2005.

[49] M. J. Khan and K.-S. Hong, "Hybrid EEG-fNIRS-based eight-command decoding for BCI: Application to quadcoptor control," *Front. Neurorobot.*, vol. 11, pp. 6-1—6-13, Feb. 2017.

[50] M. Rehan, N. Iqbal, and K.-S. Hong, "Delay-range-dependent control of nonlinear time-delay systems under input saturation," *Int. J. Robust Nonlinear Control*, vol. 26, no. 8, pp. 1647–1666, May 2016.

[51] E. Buckingham, "On physically similar systems," *Phys. Rev.*, vol. 4, no. 4, pp. 345–376, 1914.

[52] B. R. Munson, D. F. Young, and T. H. Okiishi, *Fundamentals of Fluid Mechanics*. Hoboken, NJ, USA: Wiley, 2002.

[53] G. Murphy, "Applications of similitude to the structural mechanics of reactors," *Nucl. Eng. Des.*, vol. 19, no. 1, pp. 199–206, 1972.

[54] N. G. Park, H. Rhee, H. Moon, Y. K, Jang, S. Y. Jeon, and J. I. Kim, "Modal testing and model updating of a real scale nuclear fuel rod," *Nucl. Eng. Technol.*, vol. 41, no. 6, pp. 821–830, Aug. 2009.

[55] L. Meirovitch, *Analytical Methods in Vibrations*. New York, NY, USA: Macmillan, 1967.

[56] T. Singh and H. Alli, "Exact time-optimal control of the wave equation," *J. Guid. Control Dyn.*, vol. 19, no. 1, pp. 130–134, Jan./Feb. 1996.

[57] B. Wie and R. L. Bryson, "Modeling and control of flexible space structures," in *Proc. 3rd Conf. Dyn. Control Large Struct.*, Jun. 1981, pp. 153–174.

[58] S. Yang and M. Tomizuka, "Adaptive pulse width control for precise positioning under the influence of stiction and coulomb friction," *J. Dyn. Syst. Meas. Control, Trans. ASME*, vol. 110, no. 3, pp. 221–227, Sep. 1988.

[59] D. B. Rathbun, "Pulse modulation control for flexible systems under the influence of nonlinear friction," Ph.D. dissertation, Dept. Elect. Eng., Univ. Washington, Seattle, WA, USA, 2001.

[60] J. J. Kim and T. Singh, "Controller design for flexible systems with friction: Pulse amplitude control," *J. Dyn. Syst. Meas. Control, Trans. ASME*, vol. 127, no. 3, pp. 336–344, Sep. 2005.

Umer Hameed Shah (S'16) received the B.E. and M.S. degrees in mechanical engineering from the National University of Sciences and Technology, Islamabad, Pakistan, in 2005 and 2012, respectively. He is currently working toward the Ph.D. degree in mechanical engineering with the School of Mechanical Engineering, Pusan National University, Busan, South Korea.

His research interests include dynamics and vibration control of multibody and distributed parameter systems.

Mr. Shah received the Outstanding Paper Award from the International Control Conference of the Chinese Automatic Control Society, Taiwan, in 2015.

Keum-Shik Hong (S'87–M'91–SM'10) received the B.S. degree in mechanical design and production engineering from Seoul National University, Seoul, South Korea, in 1979; the M.S. degree in mechanical engineering from Columbia University, New York, NY, USA, in 1987; and the M.S. degree in applied mathematics and the Ph.D. in mechanical engineering from the University of Illinois at Urbana–Champaign, Champaign, IL, USA, in 1991.

In 1993, he joined the School of Mechanical Engineering, Pusan National University (PNU), Busan, South Korea, where he became a Professor in 2004. His Integrated Dynamics and Control Laboratory was designated as a National Research Laboratory by the Ministry of Education, Science, and Technology (MEST) of Korea in 2003. In 2009, under the auspices of the World Class University Program of the MEST of Korea, he established the Department of Cogno-Mechatronics Engineering, PNU. His current research interests include nonlinear systems theory, brain–computer interface, adaptive control, distributed parameter systems, autonomous systems, and innovative control applications in brain engineering.

Dr. Hong served as the Editor-in-Chief of the *Journal of Mechanical Science and Technology* from 2008 to 2011, as an Associate Editor for *Automatica* from 2000 to 2006, and as the Deputy Editor-in-Chief for the *International Journal of Control, Automation, and Systems* from 2003 to 2005. He also served as the President of the Institute of Control, Robotics, and Systems (ICROS) in 2015 and is a Vice President of the Asian Control Association. He is an ICROS Fellow and a member of the ASME, the ICROS, the KSME, the KSPE, the KIEE, the KINPR, and the National Academy of Engineering of Korea. He has received many awards including the Presidential Award of Korea in 2007, the ICROS Achievement Award in 2009, the IJCAS Contribution Award in 2010, and the IEEE Academic Award of ICROS in 2016.

Sang-Hei Choi received the B.S. degree in civil and environment engineering from Korea University, Seoul, South Korea, in 1992; the M.S. degree in urban engineering from Yonsei University, Seoul, in 2006; and the Ph.D. degree in management engineering from Korea University, in 2014.

In 1995, he joined the Korean Maritime Institute, Busan, South Korea, where he is currently a Principle Researcher. Since then, he has been involved in numerous research projects including productivity improvement of both container and general-purpose terminals, layout design of a next-generation port handling system, etc. His current research interests include innovative technologies for highly efficient and intelligent port handling systems, next-generation port design, mobile harbor, and energy-efficient automated vehicles in yards.